

Synthesis and physical property studies of cyclometalated Pt(II) and Pd(II) complexes with tridentate ligands containing pyrazole and pyridine groups



Keerthika Kumarasamy, Tamiloli Devendhiran, Mei-Ching Lin*, Chi-Wen Chiu

Department of Applied Chemistry, Chaoyang University of Technology, Taichung City 413310, Taiwan, ROC

ARTICLE INFO

Article history:

Received 9 February 2020

Accepted 6 September 2020

Available online 18 September 2020

Keywords:

Tridentate ligands

Pyridine and Pyrazole

Pd(II) and Pt(II) complexes

Physical property studies

ABSTRACT

Novel substituted tridentate ligands, which contains a series of pyrazole and pyridine groups as donors, and their cyclometalated complexes have been successfully synthesized. The ligands and complexes were completely characterized by a variety of techniques, such as ^1H NMR, UV–Vis, FT-IR, mass spectrometry and elemental analysis. Meanwhile, the single crystal structures of ligand **7** and complex **11** were determined by X-ray crystallography. For ligand **7**, due to the effect of delocalization, the C(6)–C(7) bond length in the pyrazole ring is 0.05 Å shorter than a normal C–C bond. After coordinating with the metal centre, the configuration was limited by the coordination sphere, so the bond lengths and bond angles of complex **11** are different from those of ligand **7**. Through photoluminescence in acetonitrile solution at ambient temperature, two emission bands have been found between 500 and 600 nm for complexes **9** and **10**. Moreover, there are several absorbing bands respectively located at 240 to 250 nm and 300 to 310 nm for ligands **7** and **8** ($\pi(\text{L}) \rightarrow \pi^*(\text{L})$ and $n \rightarrow \pi^*(\text{L})$). A red-shift was observed in the UV spectra, on comparing the complexes with electron-donating and electron-withdrawing groups on the ligand, which is due to the electronic effect of the substituent. One absorbing band is also found at 375 to 425 nm for complexes **9** and **10**, and this band is attributed to a MLCT ($d\pi(\text{Pt}) \rightarrow \pi^*(\text{L})$).

© 2020 Elsevier Ltd. All rights reserved.

1. Introduction

Cyclometalation of d^8 transition metal complexes has recently experienced an increasing research interest; especially in palladium(II) and platinum(II) based complexes [1]. Lately, scientists have focused their research on the synthesis and application of multidentate metal chelates [2]. Therefore, the synthesis and application of multidentate metal chelates have gradually received attention, especially in the field of multidentate ligands [3]. Generally, pincer complexes illustrate the backbone of catalytic processes and this is especially true in the case of the catalytic formation of C–C bonds. The chelation of metal centers mostly use strong and efficient catalysts, where pincer compounds are unique [4]. Recently, the advantages of pincer compounds have been used in the catalytic production of C–C, C–O, C–N, C–S and C–B bonds. In coordination chemistry, many pyrazole derivatives are used as ligands. Over the past two-three decades, compounds containing two and more pyrazole fragments have gained particular popularity as they formed the basis for different metal

complexes. The presence of a nitrogen atom improves the catalytic activity, which results in the formation of higher donating ligands [5,6]. Cyclometalation in platinum metal complexes often uses bidentate or tridentate ligands to stabilize the structure, such as bipyridine (N, N) and terpyridine (N, N, N) ligands [7]. The nature of these coordination groups and their interaction with the metal centers also help generate the variety of spectroscopic properties of the different cyclometalated systems [8]. A group of coordination functional groups, such as amino [9], iminyl [10], pyridyl [11], pyrazolyl [12], phosphinyl [13] and thiol [14], have been used to maintain and stabilize the metal center for cyclometalation [15]. In recent years, cyclometalated ligands with π -conjugated bidentate and tridentate systems have considerably increased attention due to the outstanding photophysical properties of their cyclometalated Pt(II) and Pd(II) complexes. The square-planar d^8 cyclometalated complexes also have special properties for substrate binding and chemosensing [16,17].

Most of these molecules have significant photophysical and photochemical properties [17], which make them useful in applications requiring photocatalysis [18,19], photovoltaic devices [16,20–21], DNA and protein binding [22], cation detection [23,24], pH sensing [7,25] and cyano-halide detection [26], among

* Corresponding author.

E-mail address: mavis@cyut.edu.tw (M.-C. Lin).

others [24,25]. In particular, palladium(II) and platinum(II) luminescent complexes with oligopyridine [27] and cyclometallated ligands have recently been widely studied [29].

These metal complexes affect the strong light-emitting properties and the color of substances [30], which are photophysical and photochemical properties, respectively [28,31], because they have rich and diverse electron transfer processes, such as IL (intra-ligand: $\pi \rightarrow \pi^*$) and MLCT (metal–ligand charge transfer) ($d\pi \rightarrow p\pi^*$). These properties could be applied for cold sensors, increasing the interest in these areas [8,32,33]. In recent years, scientists have discovered that platinum(II) diamine compounds have luminescence properties at room temperature and that there is a long-term excited state in solution [34].

The objective of this study is to synthesize the tridentate ligands **7** and **8**, containing pyrazole, pyridine and benzene rings. The C, N, N- cyclometalated ligands **7** and **8** (Fig. 1), containing C-phenyl, N-pyridyl and N-pyrazolyl donors and where the 1-pyrazolyl-NH group can provide additional coordination, can form a variety of bonding modes [8]. Because 1-pyrazolyl-NH is a relatively easy reaction site, it can coordinate in the cyclometallic compound and facilitate other chemical reactions. It also has the characteristics of ligands that easily form cyclic metal compounds and can even form more diverse networked compounds [35]. For most tridentate cyclometalated complexes, substitution of an ancillary ligand is most common because in comparison to the direct derivation of the cyclometalating ligand, which involves a multi-step synthesis, the use of ancillary ligands is an easier approach to functionalization [35,36]. In this system, C, N, N_{pyrazolyl}, both the ancillary and cyclometalating ligands are available for easy derivatization and this approach may be more flexible towards the functionalization and integrity of cyclometalated complexes with advanced catalytic and spectroscopic properties for use in supramolecular devices and materials. Here, the pyrazolyl moiety acts as a donor group, thus the ligands mainly involve N1-substituted pyrazoles. The 1-pyrazolyl-NH group is thus not

involved and hence it does not possess any special properties in the ligand [11].

The HN-N moiety, through 1-pyrazolyl-NH, will be able to form more cyclometallic compounds with different characteristics, such as deprotonation with trimethylamine [11], formation of a binuclear metal complex via the pyrazolyl nitrogen atom [37,38]. The formation of pyrazolyl after deprotonation can be degraded to an electrophilic functional group, which can generate a bond with another metal center between molecules. Due to resonance, the pyrazole group will be more stable and the configuration of the compound can be controlled by adjusting the pH. Therefore, these compounds are being widely used as ligands [39,40].

A series of tridentate ligands and metal complexes were prepared with palladium and platinum as the central metals. Functional groups were modified at the ring positions, and the effects of the functional groups on the optical and physical properties of the complexes were investigated.

2. Experimental

2.1. Materials and methods

All experiments and manipulations were conducted under an inert nitrogen atmosphere using standard vacuum techniques. The starting materials used in this study were obtained from commercial sources and the solvents used were of analytical grade. The melting points were determined on a MP-ID. The UV–Vis spectra were recorded with a PERKIN ELMER Lambda 20 Ultraviolet–Visible spectrometer in acetonitrile solution. Fluorescence spectra were recorded on a JASCO FP-750 fluorimeter. Fourier Transform Infrared (FT-IR) spectra were recorded as potassium bromide (KBr) pellets on a Paragon 500 instrument PERKIN ELMER. ¹H NMR spectra were recorded at 298 K on VARIAN 200 MHz and BRUKER 500 MHz spectrometers using DMSO *d*₆ and CDCl₃ as sol-

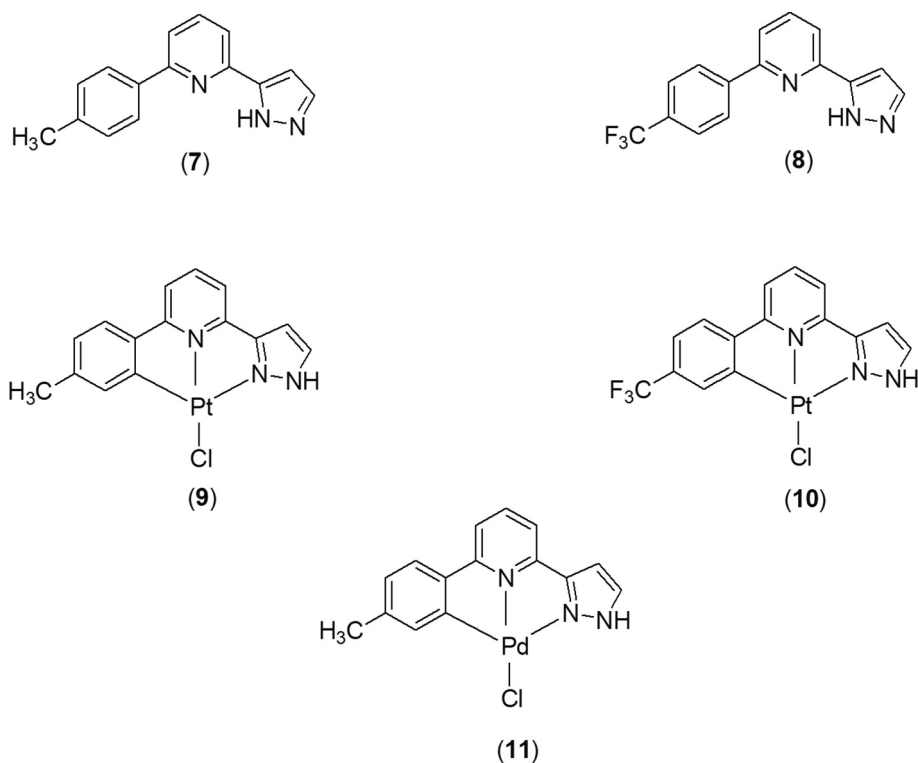


Fig. 1. Chemical structures of the pyrazole containing C,N,N ligands and their cyclometalated complexes.

vents. Elemental analyses were performed on an Elementary Vario EL III elemental analyzer. Mass spectra were recorded on a Finnigan/Thermo Quest MAT 95XL mass spectrometer.

2.2. Synthesis of compound 2

5.537 g (0.02 mol) of compound **1** was dissolved in 45 mL dry ether under nitrogen by stirring 18 mL (0.02 mol) of *n*-BuLi was added at $-78\text{ }^{\circ}\text{C}$, followed by stirring for 30 min. Next, 3 mL dimethylacetamide (0.02 mol) was slowly added at this temperature. After returning to room temperature, the reaction mixture was stirred for 17 h. The resulting mixture turned khaki yellow. The reaction product was extracted with diethyl ether and saturated NH_4Cl , then dried over Na_2SO_4 . The product was filtered, concentrated by evaporating under vacuum and purified by column techniques with 8:2 hexane/EA as the eluent, where it gave a colorless powder. Yield: 74.62%. Melting point: $44\text{ }^{\circ}\text{C}$. ^1H NMR (200 MHz, CDCl_3) δ , ppm: 8.010 ($J = 6.8\text{ Hz}$, dd, 1H), 7.697–7.664 (m, 2H), 2.705 (s, 3H, CH_3).

2.3. Synthesis of compound 3

2.07 g (0.01 mol) of compound **2** was dissolved in dry xylene (80 mL) and 1.80 g (0.015 mol) 4-methylphenylboronic acid was added under nitrogen, then 0.50 g $\text{Pd}(\text{PPh}_3)_4$ (5% mol) and 2.71 g (0.02 mol) of potassium carbonate were added. The reaction mixture was refluxed for 5 h at $100\text{ }^{\circ}\text{C}$ and monitored by TLC. Once the reaction completed, it was extracted with H_2O and CH_2Cl_2 and dried over MgSO_4 . Next it was filtered, evaporated under vacuum and then purified by column techniques with hexane/EA (9:1) as the eluent. It yielded a white powder. Yield: 91.2%. Melting point: $70\text{ }^{\circ}\text{C}$. ^1H NMR (500 MHz, CDCl_3) δ , ppm: 7.996 ($J = 8.5\text{ Hz}$, d, 2H), 7.936–7.815 (m, 3H), 7.307 ($J = 8\text{ Hz}$, d, 2H), 2.810 (s, 3H), 2.417 (s, 3H). MS(EI): 211.2 (M^+). Elemental analysis ($\text{C}_{14}\text{H}_{13}\text{NO}$); Theoretical: C, 79.59; H, 6.20; N, 6.63. Actual: C, 79.66; H, 6.52; N, 6.60%. The NMR and mass spectra are shown in the [supplementary materials](#).

2.4. Synthesis of compound 4

0.3 g (1.5 mmol) of compound **2** was dissolved in dry xylene (20 mL) and 0.431 g (2.28 mmol) 4-(trifluoromethyl)phenylboronic acid was added under nitrogen, followed by the addition of 0.091 g of $\text{Pd}(\text{PPh}_3)_4$ (5% mol) and 0.427 g (3 mmol) of potassium carbonate. The reaction mixture was refluxed for 24 hrs at $100\text{ }^{\circ}\text{C}$ and monitored by TLC. Once the reaction completed, it was extracted with H_2O and CH_2Cl_2 and dried over MgSO_4 . Next it was filtered, evaporated under vacuum and purified by column techniques with hexane/EA (9:1) as the eluent. It yielded an off-white powder ([Scheme 1](#)). Yield: 79.74%. Melting point: $76\text{ }^{\circ}\text{C}$. ^1H NMR (500 MHz, CDCl_3) δ , ppm: 8.220 ($J = 8\text{ Hz}$, d, 2H), 8.047–7.940 (m, 3H), 7.775 ($J = 8.2\text{ Hz}$, d, 2H), 2.826 (s, 3H). MS (EI): 265.1 (M^+). Elemental analysis ($\text{C}_{14}\text{H}_{10}\text{F}_3\text{NO}$): Theoretical: C, 63.40; H, 3.80; N, 5.28. Actual: C, 63.84; H, 3.58; N, 5.06%. The NMR and mass spectra are shown in the [supplementary materials](#).

2.5. Synthesis of compound 5

0.492 g (2.3 mmol) of compound **3** was dissolved in *N*, *N*-dimethylformamide dimethyl acetal (1.2 mL, 8.9 mmol). The solution was refluxed for an hour at $100\text{ }^{\circ}\text{C}$ and monitored by TLC. Once the reaction completed, it was cooled, evaporated under vacuum and purified by column techniques, with CH_2Cl_2 /hexane (1:1) as the eluent. This yielded a pale yellow powder which was recrystallized using CH_2Cl_2 and hexane to obtain pale yellow crystals. Yield: 87.8%. Melting point: $151.5\text{ }^{\circ}\text{C}$. ^1H NMR (500 MHz,

CDCl_3) δ , ppm: 8.079 ($J = 7.5\text{ Hz}$, d, 1H), 7.997 ($J = 8\text{ Hz}$, d, 2H), 7.950–7.774 (m, 3H), 7.303 ($J = 8\text{ Hz}$, d, 2H), 3.171 (s, 3H), 3.015 (s, 3H), 2.416 (s, 3H). MS (EI): 266.3 (M^+). Elemental analysis ($\text{C}_{17}\text{H}_{18}\text{N}_2\text{O}$), Theoretical: C, 76.66; H, 6.81; N, 10.52; Actual: C, 77.06; H, 6.54; N, 10.45%. The NMR and mass spectra are shown in the [supplementary materials](#).

2.6. Synthesis of compound 6

0.42 g (1.61 mmol) of compound **4** was dissolved in *N*, *N*-dimethylformamide dimethyl acetal (100 mL, 8.9 mmol). The resulting solution was refluxed for 18 hrs at $100\text{ }^{\circ}\text{C}$ and monitored by TLC. Once the reaction completed, it was cooled, evaporated under vacuum and purified by column techniques with CH_2Cl_2 /hexane (1:1) as the eluent. It yielded an off-white powder which was recrystallized using CH_2Cl_2 and hexane to obtain white needle crystals. Yield: 80.8%. Melting point: $155\text{ }^{\circ}\text{C}$. ^1H NMR (500 MHz, CDCl_3) δ , ppm: 8.220–8.146 (m, 3H), 7.988–7.816 (m, 3H), 7.772 ($J = 8.2\text{ Hz}$, d, 2H), 6.673 ($J = 13\text{ Hz}$, d, 1H), 3.191 (s, 3H), 3.047 (s, 3H). MS (EI): 320 (M^+). Elemental analysis ($\text{C}_{17}\text{H}_{15}\text{F}_3\text{N}_2\text{O}$), Theoretical: C, 63.75; H, 4.72; N, 8.75; Actual: C, 63.19; H, 4.90; N, 8.72%. The NMR and mass spectra are shown in the [supplementary materials](#).

2.7. Synthesis of ligand 7

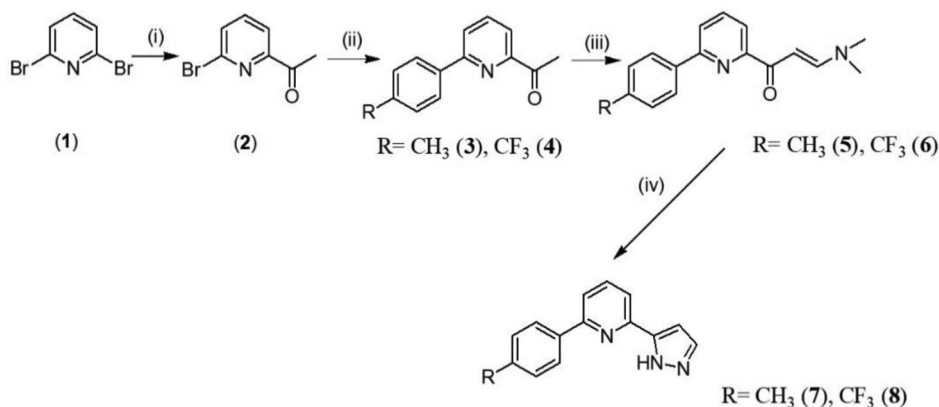
1.51 g (5.6 mmol) of compound **5** was dissolved in ethanol (2 mL). 80% Hydrazine hydrate (2.6 mL) was added and the resulting solution was refluxed for 4 hrs at $65\text{ }^{\circ}\text{C}$. The solution was poured into 200 mL of water and it produced a white turbid precipitate, which was filtered, dried and purified by column techniques with dichloromethane/hexane as the eluent. It yielded a yellow powder which was recrystallized using dichloromethane/hexane to obtain pale yellow needle crystals. Yield: 97.3%. Melting point: $160\text{ }^{\circ}\text{C}$. ^1H NMR (500 MHz, CDCl_3) δ , ppm: 7.957 ($J = 8.5\text{ Hz}$, d, 2H), 7.756 ($J = 16\text{ Hz}$, t, 1H), 7.649–7.616 (m, 2H), 7.591 ($J = 7\text{ Hz}$, d, 1H), 7.292 ($J = 8\text{ Hz}$, d, 2H), 6.803 (s, 1H), 2.40 (s, 3H). MS (EI): 235.1 (M^+), 236.1 ($\text{M} + 1$). Elemental analysis ($\text{C}_{15}\text{H}_{13}\text{N}_3$), Theoretical: C, 76.57; H, 5.57; N, 17.86; Actual: C, 76.00; H, 5.46; N, 17.60%. The NMR and mass spectra are shown in the [supplementary materials](#).

2.8. Synthesis of ligand 8

0.41 g (1.28 mmol) of compound **6** was dissolved in ethanol (3 mL). 80% Hydrazine hydrate (1.3 mL) was added and the resulting solution was refluxed for 4 hrs at $65\text{ }^{\circ}\text{C}$. The solution was poured into 200 mL of water and it produced a white turbid precipitate, which was filtered, dried and purified by column techniques with dichloromethane/hexane as the eluent. It yielded a yellow powder which was recrystallized using dichloromethane/hexane to obtain pale yellow needle crystals. Yield 92.3%. Melting point: $173\text{ }^{\circ}\text{C}$. ^1H NMR (500 MHz, CDCl_3) δ , ppm: 8.168 ($J = 8.2\text{ Hz}$, d, 2H), 7.813 ($J = 15.2\text{ Hz}$, t, 1H), 7.732–7.646 (m, 5H), 6.876 (s, 1H). MS (EI): 289.1 (M^+). Elemental analysis ($\text{C}_{15}\text{H}_{10}\text{F}_3\text{N}_3$); Theoretical: C, 62.28; H, 3.48; N, 14.53; Actual: C, 62.25; H, 4.01; N, 14.68%. The NMR and mass spectra are shown in the [supplementary materials](#).

2.9. Synthesis of complex 9

A mixture of ligand **7** (0.21 g, 0.9 mmol) and K_2PtCl_4 (0.383 g, 0.9 mmol) was dissolved in glacial acetic acid (25 mL). The resulting solution was refluxed for 24 h, whereupon it formed a yellow precipitate. The precipitate was filtered, washed with H_2O , $\text{C}_2\text{H}_5\text{OH}$, CH_3OH and ether as washing liquids, and then dried. It



Scheme 1. Synthesis of the new substituted C, N, N_{pyrazolyl} ligands: (i) *n*-BuLi, *N,N*-dimethylacetamide, ethyl ether, $-78\text{ }^{\circ}\text{C}$; (ii) substituted phenylboronic acid in xylene, Pd(PPh₃)₄, potassium carbonate, R = CH₃, CF₃, $100\text{ }^{\circ}\text{C}$, 24 h; (iii) *N,N*-dimethylformamide dimethyl acetal, reflux, 18 h; (iv) N₂H₄, EtOH, $70\text{ }^{\circ}\text{C}$, 4 h.

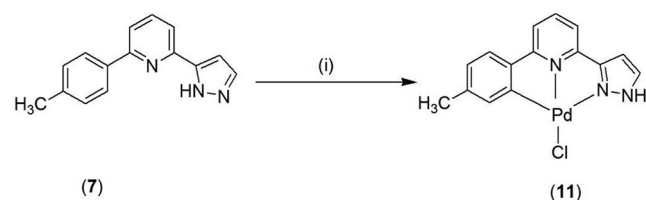
yielded a yellow powder which was recrystallized using acetone and CH₃OH (Scheme 2). Yield: 64.26%. ¹H NMR (200 MHz, DMSO *d*₆) δ , ppm: 8.137 (s, 1H), 7.989 (*J* = 15.8 Hz, t, 1H), 7.784 (*J* = 16.2 Hz, t, 2H), 7.415 (*J* = 7.8 Hz, s, 1H), 7.311 (s, 1H), 7.187 (s, 1H), 6.862 (*J* = 7.8 Hz, d, 1H), 2.260 (s, 3H). MS (FAB): 465 (M⁺). The NMR and mass spectra are shown in the [supplementary materials](#).

2.10. Synthesis of complex 10

A mixture of ligand **8** (0.26 g, 0.9 mmol) and K₂PtCl₄ (0.381 g, 0.9 mmol) was dissolved in glacial acetic acid (25 mL). The resulting solution was refluxed for 24 h, whereupon it formed a yellow precipitate. This precipitate was filtered, washed with H₂O, C₂H₅OH, CH₃OH and ether as washing liquids, and then dried. It yielded a yellow solid which was recrystallized using acetonitrile and ether. Yield: 55.2%. MS (FAB): 520 (M + 1). ¹H NMR (200 MHz, DMSO *d*₆) δ , ppm: 8.150 (s, 1H), 8.096 (*J* = 15.8 Hz, t, 1H), 7.887 (*J* = 7.8 Hz, d, 2H), 7.766 (*J* = 5.6 Hz, d, 1H), 7.698 (s, 1H), 7.359 (*J* = 7.6 Hz, d, 1H), 7.211 (s, 1H). The NMR and mass spectra are shown in the [supplementary materials](#).

2.11. Synthesis of complex 11

A mixture of ligand **7** (0.1181 g, 0.5 mmol) and K₂PdCl₄ (0.1624 g, 0.5 mmol) was dissolved in acetonitrile (15 mL) and water (15 mL). The resulting solution was refluxed for 18 hrs at $75\text{ }^{\circ}\text{C}$, then cooled, evaporated under vacuum, and then extracted with CH₂Cl₂ and dried over MgSO₄. After that, it was filtered and evaporated under vacuum, adding an appropriate amount of ether to produce a yellow powdered solid. Recrystallized from acetonitrile and ether resulted in pale yellow needle crystals (Scheme 3). ¹H NMR (200 MHz, DMSO *d*₆) δ , ppm: 8.073 (*J* = 5.4 Hz, d, 2H), 7.799 (*J* = 7.8 Hz, d, 2H), 7.491 (*J* = 7.8 Hz, s, 1H), 7.372 (s, 1H),



Scheme 3. Synthesis of the cyclopalladated complex: (i) K₂PdCl₄, acetonitrile/ H₂O, reflux, 24hr.

7.172 (s, 1H), 6.911 (*J* = 8 Hz, d, 1H)). The NMR spectrum is shown in the [supplementary materials](#).

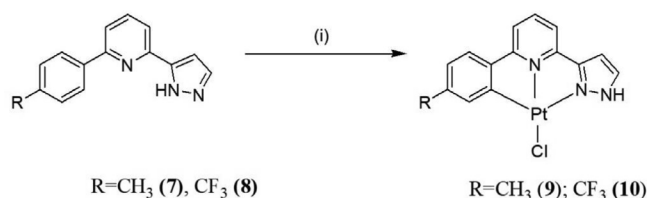
2.12. Crystal structure determination

Intensity data were collected at room temperature on a Bruker Axs SMART 1000 CCD diffractometer, using a molybdenum (Mo) target ($\lambda = 0.71069\text{ \AA}$) as the radiation source and θ - 2θ angle as the scanning pattern. Data collections were processed with SAINT software. Absorption data corrections were applied by using the SADABS [41] software package. The structures of the ligand and complex were solved by direct methods using SHELXTL [42] with standard difference Fourier syntheses. All non-hydrogen atoms of ligand **7** and complex **11** were purified with anisotropic displacement parameters. The crystal data and structural clarification details for ligand **7** and complex **11** are shown in Table 1.

3. Results and discussion

3.1. Synthesis and characterization

The new cyclometalated ligands **7** and **8** were synthesized following the procedure shown in Scheme 1. Compound **1** was reacted with *n*-BuLi and *N,N*-dimethylacetamide via lithiation at a low temperature and the bromine group on one side was substituted by a keto group to obtain compound **2**. A palladium-catalyzed (Pd) Suzuki cross-coupling reaction with substituted phenylboronic acid was performed to synthesize compounds **3** and **4** (ketone) from compound **2**. These compounds were converted into the intermediate compounds **5** and **6** by refluxing with *N,N*-dimethylformamide dimethyl acetal. These resulting ketones were obtained after purification by column chromatography and recrystallization. The C, N, N_{pyrazolyl} ligand derivatives (**7** and **8**) were conveniently prepared in excellent yields by the



Scheme 2. Synthesis of the cycloplatinated complex: (i) K₂PtCl₄, glacial acetic acid, reflux, 24hr.

Table 1
Crystal data and structure refinement details for **7** and **11**.

| Parameter | 7 | 11 |
|--|--|--|
| Empirical formula | C ₁₅ H ₁₃ N ₃ | C ₁₅ H ₁₄ ClN ₃ OPd |
| Formula weight | 235.28 | 394.14 |
| Temperature, K | 297(2) | 297(2) |
| Wavelength, Å | 0.71073 | 0.71073 |
| Crystal system | Orthorhombic | Monoclinic |
| Space group | P b c a | P 21/n |
| Unit cell dimensions | | |
| a, Å | 14.8511(11) | 5.8803(4) |
| α, ° | 90 | 90 |
| b, Å | 8.4187(6) | 15.0753(10) |
| β, ° | 90 | 98.8100(10) |
| c, Å | 19.9196(14) | 16.4779(11) |
| γ, ° | 90 | 90 |
| Volume, Å ³ | 2490.5(3) | 1443.49(17) |
| Z | 8 | 4 |
| Density (calc.), Mg/m ³ | 1.255 | 1.814 |
| Absorption coefficient, mm ⁻¹ | 0.077 | 1.472 |
| F(000) | 992 | 784 |
| Crystal size, mm ³ | 0.76 × 0.60 × 0.50 | 0.85 × 0.32 × 0.30 |
| Theta range for data collection, ° | 2.04 to 26.02 | 1.84 to 26.02 |
| Index ranges | -18 ≤ h ≤ 17, -10 ≤ k ≤ 7, -21 ≤ l ≤ 24 | -7 ≤ h ≤ 4, -15 ≤ k ≤ 18, 16 ≤ l ≤ 20 |
| Reflections collected | 13,020 | 7969 |
| Independent reflections | 2452 [R(int) = 0.0296] | 2839 [R(int) = 0.0286] |
| Completeness to theta = 26.02° | 99.9% | 99.8% |
| Absorption correction | Empirical | Empirical |
| Max. and min. transmission | 1.000000 and 0.710106 | 0.6665 and 0.3677 |
| Refinement method | Full-matrix least-squares on F ² | Full-matrix least-squares on F ² |
| Data / restraints / parameters | 2452 / 0 / 179 | 2839 / 2 / 201 |
| Goodness-of-fit on F ² | 1.037 | 1.031 |
| Final R indices [I > 2σ(I)] | R1 = 0.0383, wR2 = 0.1022 | R1 = 0.0296, wR2 = 0.0827 |
| R indices (all data) | R1 = 0.0478, wR2 = 0.1110 | R1 = 0.0326, wR2 = 0.0863 |
| Largest diff. peak and hole, e Å ⁻³ | 0.164 and -0.171 | 0.783 and -0.863 |

condensation of the resulting compounds **5** and **6** with hydrazine under basic conditions.

The neutral cycloplatinated complexes **9** and **10** were obtained in over 60% yields by refluxing the corresponding ligands with K₂PtCl₄ in an equimolar ratio under acidic conditions. Similarly, the neutral cyclopalladated complex **11** was obtained by refluxing the corresponding ligand with K₂PdCl₄ in an equimolar ratio in acetonitrile/water for 24 h. The analytical data of the platinum(II) and palladium(II) complexes are in good agreement with the molecular structures proposed.

The FT-IR spectra of the pyrazolyl ligands **7** and **8** showed medium to strong bands in the region 3241–3230 cm⁻¹, which indicates N–H functional groups. The C=O stretching vibrations were not observed in the ligands due to cyclization of the pyrazole group. This is further supported by the appearance of new bands in the region 1640 cm⁻¹, which might be C=N fragments. (Figs. S21–S26, supplementary materials). Upon complexation, the bands associated with N–H and C=N stretching frequencies appeared and shifted to lower frequencies by 27–35 cm⁻¹ and this denotes that the ligands coordinate with the metal through C, N and N atoms. Hence these shifts confirmed the coordination of the ligand to the palladium metal.

The bonding arrangement is further supported by the ¹H NMR spectra of ligands **7** and **8**; all the aromatic protons appeared as multiplets in the region around δ 8.16–6.87 ppm. In ligand **7**, the aromatic methyl proton also appeared as a singlet in the region around δ 2.40 ppm. In addition, the two singlet peaks around δ

3.19 and 3.01 ppm for -N(CH₃)₂ disappeared in both ligands, and the doublet for the C=C peaks around δ 6.68 ppm also disappeared due to cyclization of pyrazole group, followed by dehydration to form an imine, indicating the formation of a pyrazole ring. After cyclization, the pyrazole N–H might be exchanged with a deuterated solvent, due to which the -NH hydrogen signal is not observed in the NMR spectrum (Figs. S1–S6, supplementary materials).

This observation was further proven with a ¹H–¹H 2D NMR spectrum. In this spectrum, the middle hydrogen atom on the pyridine ring has a peak at δ 7.75 ppm and it splits into triplet due to the influence of the adjacent carbon atoms. The pyrazole hydrogen atom peaks appear as doublets in the region δ 7.64 ppm, and the chemical shift is also moved more downfield due to the nitrogen atom. The position of the multiplets at δ 7.64–7.61 ppm indicate the hydrogen atoms on both sides of the pyridine ring. The benzene hydrogen atoms appear as doublets in the region around δ 7.95 and 7.29 ppm. At δ 7.59 and 6.80 ppm, two peaks appear which indicate the pyrazole hydrogen atoms. Ligand **8** has similar spectral properties, with slight changes in its functional group. (Figs. S9–S10, supplementary materials).

In complex **9**, the ¹H NMR spectrum clearly shows a singlet observed in the region around δ 8.13 ppm, assigned to the pyrazole ring hydrogen. The aromatic protons of the coordinated ligands appear as multiplets in the region around δ 8.13–6.86 ppm. These are magnetically downfield shifted compared with their ligands, indicating the coordination of the substituted benzene, pyridine, and pyrazole rings (C, N, N) to platinum and palladium. The aromatic methyl protons were also observed as singlets in the region δ 2.260 and 2.264 ppm. In particular, the benzene ring is uncoordinated to the platinum metal, being 1,4 substituted, and the signals are for two hydrogen atoms. If the hydrogen doublet of the benzene ring is due to coordination with the metal centre, one of the hydrogen atoms on the benzene ring will have been eliminated before it coordinates with the metal due to π-conjugation. (Figs. S7–S9, supplementary materials).

This observation was further proven with the ¹H–¹H 2D NMR spectrum for complex **9** which showed the middle hydrogen atom on the pyridine ring in the region around δ 8.727 ppm. The position of δ 8.466 ppm indicates hydrogen atoms on both sides of the pyridine ring and a doublet for the hydrogen atoms on the benzene ring were observed in the region around δ 8.178 and 7.625 ppm; also a hydrogen singlet was observed in the region δ 8.076 ppm. The benzene and pyrazole hydrogen peaks were observed in the regions δ 7.956 and 8.903 ppm. So, this proves that the complexes were successfully synthesized (Fig. S12, supplementary materials).

The EI mass spectrometer values of compounds **3**, **4**, **5**, **6** and ligands **7** and **8** are shown in Figs. S15–S20, respectively. The molecular ion peaks for ligands **7** and **8** were observed at m/z = 236.1 (M + 1) for C₁₅H₁₃N₃ and m/z = 289.1 (M + 1) for C₁₅H₁₀F₃N₃, respectively, which is in excellent agreement with the theoretical values. This proves that all the compounds and ligands were successfully synthesized.

The FAB mass spectrometer values of complexes **9** and **10** are shown in Figs. S14 and S15, respectively. The molecular ion peak for complex **9** was observed at m/z = 465 (M⁺) for C₁₅H₁₂ClN₃Pt. This is consistent with the molecular weight of the experimental formula. The molecular ion peak for complex **10** was observed at m/z = 520 (M + 1) for C₁₅H₉ClF₃N₃Pt, which is also consistent with the molecular weight of the experimental formula. Thus, this proves that the complexes were successfully synthesized.

3.2. Structural analysis of the compounds

3.2.1. Structure analysis of ligand **7**

Single crystals of ligand **7** grew effectively by evaporation of CH₃CN/ether solutions. Fig. 2 shows the perspective view of the

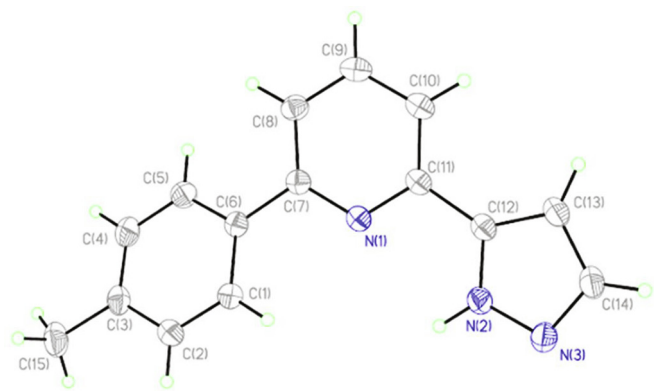


Fig. 2. Molecular structure of ligand **7** showing the atom labelling scheme.

crystal structure. A summary of the data collection and refinement parameters of ligand **7** and complex **11** is listed in Table 1 and selected bond lengths and bond angles are listed in Table 2. The C(4)–C(5) bond length is 1.379 Å, which is similar to the average value of the C–C bond in a benzene ring (1.385 Å). The C(8)–C(9) bond length is 1.375 Å, which is similar to the average value of the C–C bond on a pyridine ring (1.369 Å). The common bond length in a pyrazole ring is 1.356 Å. Generally, the C–C bond length is 1.54 Å, but due to the influence of electron delocalization, the C(13)–C(14) bond length (1.384 Å) is shorter than the general C–C bond length. The C(6)–C(7) and C(11)–C(12) bond lengths are 1.483 and 1.463 Å, respectively, which are shorter than the general C–C bond length, due to the delocalization of electrons. These three rings are conjugated systems. The hydrogen atom was also observed on the N(2) atom, which also proves the part that was difficult to confirm by ^1H NMR spectroscopy.

3.3. Structure analysis of complex **11**

The single crystals of complex **11** grew effectively by evaporation of a CH_3CN /ether solution. Fig. 3 shows the perspective view of the crystal structure. Selected bond lengths and bond angles are given in Table 3. The crystal lattice of complex **11** is monoclinic and the space group is $p2_1/n$. The crystal structure shows three chelate rings composed of the central palladium metal with the ligand. The position of the chloride ion bond forms a four-coordinated neutral molecule. The average benzene ring bond length is 1.393 Å, only the C(1)–C(6) bond length is longer (by about 0.03 Å more than before coordination). In the pyridine ring part, the N(1)–C(7) and N(1)–C(11) bond lengths are also longer than that before coordination, because the configuration after coordination is strained by the metal, resulting in a slight distortion. The N(1)–Pd(1)–Cl(1) bond angle is 177.60° (close to 180°), which is consistent with previous literature values [8]. The difference between the maximum and minimum values of the angle is 9.34° and after coordination the difference between the maximum and minimum bond angles is only 6.1° (Table 4). Before coordination, the pyrazole ring as a whole is closer to a regular pentagon, because when the

Table 2
Selected bond lengths (Å) and angles (deg) for ligand **7**.

| Bond lengths | | | |
|------------------|------------|------------------|------------|
| C(6)–C(7) | 1.4839(17) | N(2)–N(3) | 1.3505(16) |
| C(13)–C(14) | 1.384(2) | C(12)–N(2) | 1.3392(17) |
| Bond angles | | | |
| C(6)–C(7)–N(1) | 116.53(11) | C(11)–C(12)–N(2) | 120.55(11) |
| N(1)–C(11)–C(12) | 115.31(11) | C(1)–C(6)–C(7) | 120.45(11) |

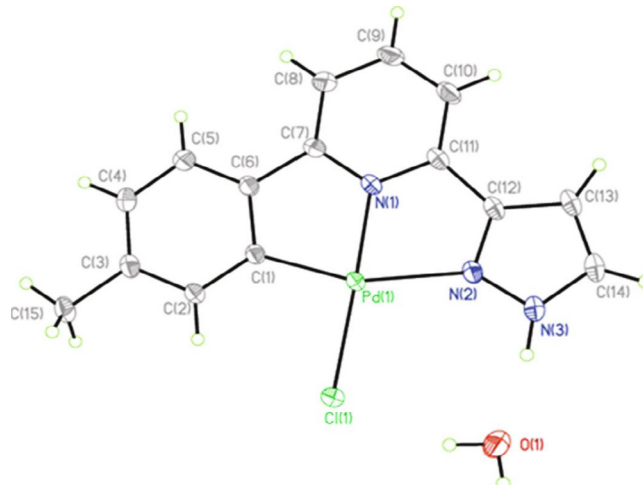


Fig. 3a. Molecular structure of complex **11** showing the atom labelling scheme.

whole ring is not bonded by the metal it is relatively free. After coordination, it is bonded by the metal, resulting in the configuration being restricted. Therefore, the phenomena of the bond angles decreasing and the bond lengths changing occur. As all the platinum(II) and palladium(II) complexes showed similar spectral properties, the other complexes are considered to have a similar structure to complex **11**. Table 5.

3.4. Spectroscopic and luminescent properties

UV–visible absorption and photoluminescence spectra were recorded in acetonitrile solutions at room temperature. Figs. 4 and 5 shows the absorption spectra of ligands **7** and **8** and complexes **9** and **10**, respectively. The emission spectra of complexes **9** and **10** are shown in Fig. 6, and the complete spectroscopic data are outlined in Table 4. Ligands **7** and **8** exhibit absorption bands at 240–250 and 300–310 nm, respectively, corresponding to $(\pi(L) \rightarrow \pi^*(L))$ and $n \rightarrow \pi^*$ ligand–ligand charge transfer transitions. From the experimental data, the electronic effect of the substituents was observed. Compared to a weakly activating compound (H) [7], when a substituent is an electron-donating group, the absorption wavelength shifts to a longer wavelength by 7 nm (from 242 nm for the H-substituted compounds), but when a substituent is an electron-withdrawing group, the absorption wavelength shifts to a shorter wavelength by 2 nm, which is around 300 nm, the change range of the absorption band is similar. So, the energy level change is very small due to the red-shift phenomenon.

Here, complexes **9** and **10** exhibit intense absorption bands in the region 410–240 nm. The absorption spectra of the cyclometalated platinum(II) complexes exhibit three strong intense absorption bands around 275–375 nm which are assigned to $(\pi(L) \rightarrow \pi^*(L))$ and $n \rightarrow \pi^*$ ligand–ligand charge transfer (LLCT) transitions. The lowest energy absorption bands appear in the region around 390 nm and are described as $(d\pi(\text{Pt}) \rightarrow \pi^*(L))$ metal–ligand charge transfer (MLCT) transitions. Both complexes show an absorption tail at 410–475 nm, which indicates a spin forbidden metal–ligand charge-transfer transition. From the experimental data, an electronic effect for the substituent is also observed. So, these complexes exhibit the longest absorption wavelength.

The variation range is from 340 to 353 nm. When comparing complex **9** to complex **10**, complex **9** displays the longest absorption wavelength in the region 353 nm and the absorption wavelength shifted to a longer wavelength by 13 nm (340 nm) for

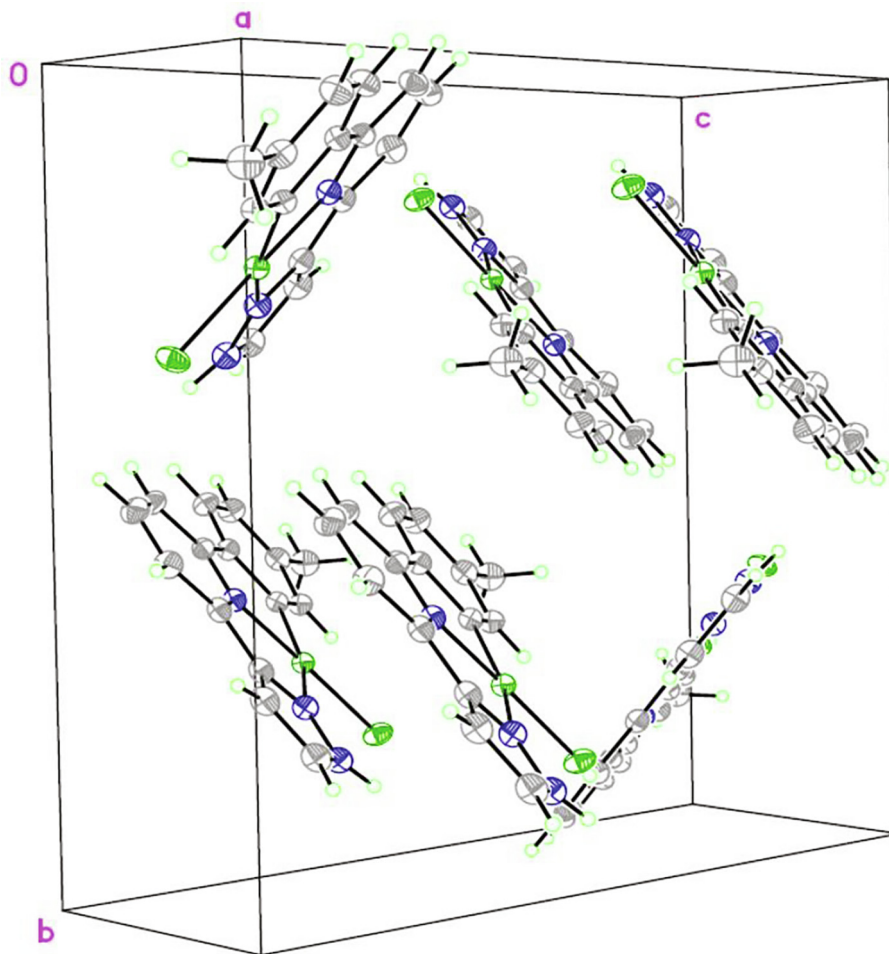


Fig. 3b. Crystal packing pattern of complex 11.

Table 3
Selected bond lengths (Å) and angles (deg) for complex 11.

| Bond lengths | | | |
|---------------|-----------|---------------|-----------|
| Pd(1)-C(1) | 1.979(2) | N(2)-N(3) | 1.342(3) |
| Pd(1)-N(1) | 1.982(2) | Pd(1)-Cl(1) | 2.3292(7) |
| Pd(1)-N(2) | 2.177(2) | | |
| Bond angles | | | |
| C(1)-Pd-N(1) | 81.57(9) | C(1)-Pd-Cl(1) | 96.50(7) |
| N(1)-Pd-N(2) | 77.49(8) | C(1)-Pd-N(2) | 159.06(9) |
| N(2)-Pd-Cl(1) | 104.43(6) | N(1)-Pd-Cl(1) | 177.60(6) |

Table 4
Selective bond lengths (Å) and bond angles (deg) before and after coordination for ligand 7 and complex 11.

| Bond lengths | Ligand 7 (Before coordination) | Complex 11 (After coordination) |
|-------------------|-----------------------------------|------------------------------------|
| C(1)-C(6) | 1.3904 | 1.419 |
| N(1)-C(7) | 1.3392 | 1.345 |
| N(1)-C(11) | 1.3457 | 1.352 |
| Bond angles | | |
| C(12)-N(2)-N(3) | 113.11 | 106.0 |
| N(2)-C(12)-C(13) | 105.95 | 110.5 |
| C(12)-C(13)-C(14) | 105.12 | 104.5 |
| C(13)-C(14)-N(3) | 112.03 | 108.4 |
| C(14)-N(3)-N(2) | 103.77 | 110.6 |
| Max-Min | 9.34 | 6.1 |

Table 5
UV-Visible absorption data of ligands 7 and 8, and complexes 9 and 10 in acetonitrile solution at ambient temperature.

| Ligands and Complexes | $\lambda/\text{nm}(\epsilon_{\text{max}}/\text{dm}^3, \text{mol}^{-1} \text{cm}^{-1})$ |
|-----------------------|--|
| 7 | 249(26373), 305(12359) |
| 8 | 240(25315), 303(10830) |
| 9 | 249(27627), 304(16720), 353(7260), 390(2060) |
| 10 | 249(19403), 301(13841), 340(5816), 391(1867) |

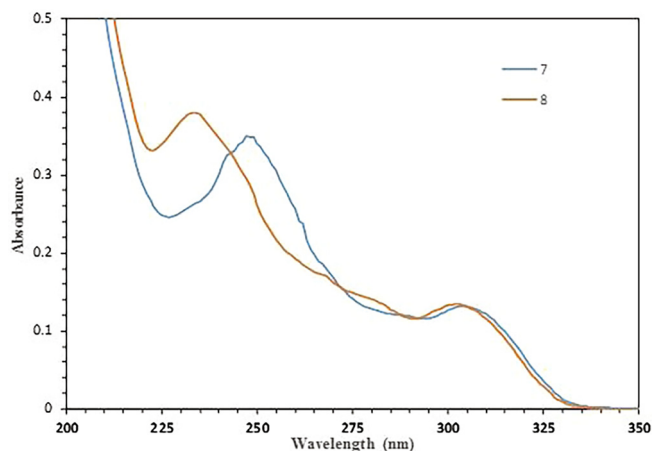


Fig. 4. UV-visible spectra of ligands 7 and 8 in acetonitrile solution at room temperature.

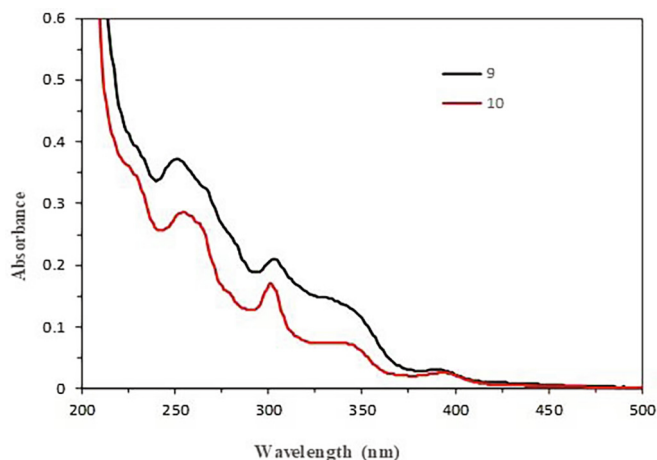


Fig. 5. UV-visible spectra of complexes **9** and **10** in acetonitrile solution at room temperature.

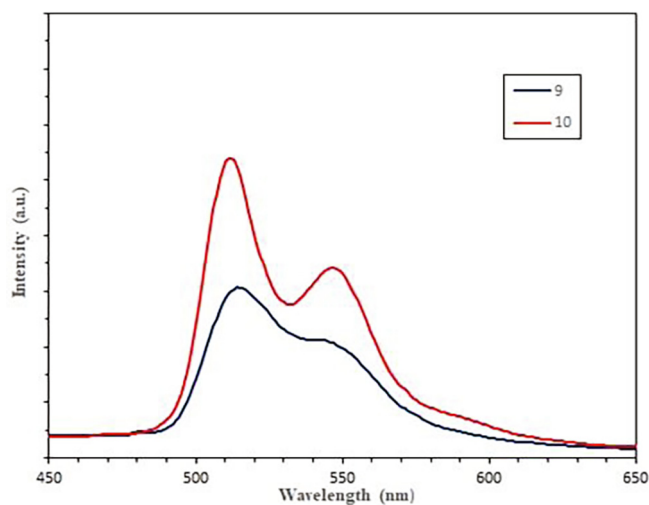


Fig. 6. PL spectra of complexes **9** and **10** in acetonitrile (10^{-4} M) solution at room temperature.

complex **10**. Thus, the CF_3 substituent results in a red-shift, due to the phenomenon of electron displacement. The pattern of the electronic spectra of complexes **9** and **10** are similar to previously reported square-planar complexes.

Complexes **9** and **10** display weak emission spectra (Fig. 6) in acetonitrile solution at ambient temperature. The emission wavelength of the complexes are in the region 500–550 nm. Complexes **9** and **10** give a weak emission peak (λ_{max}) at 516 nm. The Stokes shift explains that the emission comes from the spin-forbidden triplet excited state. On comparing the substituent of complex **9** as an electron-donating group to the substituent of complex **10** as an electron-withdrawing group, it was found that the emission wavelength shows a small red-shift phenomenon, as shown in Fig. 6.

4. Conclusions

In this investigation, we explained the design and synthesis of new substituted C, N, $\text{N}_{\text{pyrazolyl}}$ type ligands **7** and **8**, containing pyrazolyl as a donor for the cyclometalation of d^8 palladium(II) and platinum(II) centers. We investigated the structures of ligand **7** and complex **11**, together with spectroscopic studies of ligands **7** and **8**, and complexes **9** and **10**. In the structural studies, we have

observed that the bond length of the pyrazole ring, C(13)–C(14), was shorter than ordinary C–C bonds, mainly due to the effect of delocalization. In future work, we will focus on double coordination and protonation with different transition metals to explore the optical and physical properties.

CRedit authorship contribution statement

Keerthika Kumarasamy: Validation, Investigation, Resources, Data curation, Writing - original draft, Visualization. **Tamiloli Devendhiran:** Investigation, Writing - original draft. **Mei-Ching Lin:** Conceptualization, Methodology, Software, Formal analysis, Resources, Writing - original draft, Visualization, Supervision, Project administration. **Chi-Wen Chiu:** Software, Investigation, Data curation.

Declaration of Competing Interest

The authors declare that they have no known competing financial interests or personal relationships that could have appeared to influence the work reported in this paper.

Acknowledgments

We thank the Ministry of Science and Technology (MOST 98-2113-M-324-003-MY2), Taiwan for support to this research.

Appendix A. Supplementary data

Supplementary data to this article can be found online at <https://doi.org/10.1016/j.poly.2020.114799>.

References

- [1] A. Chakraborty, J.E. Yarnell, R.D. Sommer, S. Roy, F.N. Castellano, Excited-State Processes of Cyclometalated Platinum(II) Charge-Transfer Dimers Bridged by Hydroxypyridines, *Inorg. Chem.* 57 (3) (2018) 1298–1310.
- [2] J. Crasson, R. Réau, π -Conjugated phosphole derivatives: Synthesis, optoelectronic functions and coordination chemistry, *Dalton Trans.* 6865–6875 (2008).
- [3] S. Alvarez, Distortion Pathways of Transition Metal Coordination Polyhedra Induced by Chelating Topology, *Chem. Rev.* 115 (2015) 13447–13483.
- [4] D. Morales-Morales (Ed.), *Pincer Compounds: Chemistry and Applications*, Elsevier, Netherlands, 2018.
- [5] H. Valdés, M.A. García-Eleno, D. Canseco-Gonzalez, D. Morales-Morales, Recent Advances in Catalysis with Transition-Metal Pincer Compounds, *ChemCatChem* 10 (15) (2018) 3136–3172.
- [6] H. Valdés, E. Rufino-Felipe, D. Morales-Morales, Pincer complexes, leading characters in C–H bond activation processes. Synthesis and catalytic applications, *J. Organomet. Chem.* 898 (2019) 120864, <https://doi.org/10.1016/j.jorganchem.2019.07.015>.
- [7] T.A. Koizumi, T. Tomon, K. Tanaka, Terpyridine-analogous (N, N, C)-Tridentate ligands: Synthesis, structures, and electrochemical properties of ruthenium(II) complexes bearing tridentate pyridinium and pyridinylidene ligands, *Organometallics* 22 (2003) 970–975.
- [8] C.-K. Koo, Y.-M. Ho, C.-F. Chow, M.-W. Lam, T.-C. Lau, W.-Y. Wong, Synthesis and Spectroscopic Studies of Cyclometalated Pt(II) Complexes Containing a Functionalized Cyclometalating Ligand, 2-Phenyl-6-(1 H -pyrazol-3-yl)pyridine, *Inorg. Chem.* 46 (9) (2007) 3603–3612.
- [9] M.L. O'Duill, R. Matsuura, Y. Wang, J.L. Turnbull, J.A. Gurak Jr., D.-W. Gao, G. Lu, P. Liu, K.M. Engle, Tridentate Directing Groups Stabilize 6-Membered Palladacycles in Catalytic Alkene Hydrofunctionalization, *J. Am. Chem. Soc.* 139 (44) (2017) 15576–15579.
- [10] M. Albrecht, Cyclometalation using d-block transition metals: Fundamental aspects and recent trends, *Chem. Rev.* 110 (2010) 576–623.
- [11] Y.M. Ho, C.K. Koo, K.L. Wong, H.K. Kong, C.T.L. Chan, W.M. Kwok, C.F. Chow, M. H.W. Lam, W.Y. Wong, The synthesis and photophysical studies of cyclometalated Pt(II) complexes with C,N,N-ligands containing imidazolyl donors, *Dalton Trans.* 41 (2012) 1792–1800.
- [12] A.B. Tamayo, S. Garon, T. Sajoto, P.I. Djurovich, I.M. Tsyba, R. Bau, M.E. Thompson, Cationic bis-cyclometalated iridium(III) diamine complexes and their use in efficient blue, green, and red electroluminescent devices, *Inorg. Chem.* 44 (2005) 8723–8732.

- [13] A. Weisman, M. Gozin, H.-B. Kraatz, D. Milstein, Rhodium and Palladium Complexes of a 3,5-Lutidine-Based Phosphine Ligand, *Inorg. Chem.* 35 (7) (1996) 1792–1797.
- [14] M.E. Van Der Boom, D. Milstein, Cyclometalated phosphine-based pincer complexes: Mechanistic insight in catalysis, coordination, and bond activation, *Chem. Rev.* 103 (2003) 1759–1792.
- [15] K. Okamoto, T. Kanbara, T. Yamamoto, A. Wada, Pincer Platinum Complexes Derived from 3,5-Bis(anilinothiocarbonyl)toluene, *Organometallics* 25 (2006) 4026–4029.
- [16] M.K. Salomón-Flores, I.J. Bazany-Rodríguez, D. Martínez-Otero, M.A. García-Eleno, J.J. Guerra-García, D. Morales-Morales, A. Dorazco-González, Bifunctional colorimetric chemosensing of fluoride and cyanide ions by nickel-POCOP pincer receptors, *Dalton Trans.* 46 (15) (2017) 4950–4959.
- [17] W. Lu, B.X. Mi, M.C.W. Chan, Z. Hui, C.M. Che, N. Zhu, S.T. Lee, Light-Emitting Tridentate Cyclometalated Platinum(II) Complexes Containing σ -Alkynyl Auxiliaries: Tuning of Photo- and electrophosphorescence, *J. Am. Chem. Soc.* 126 (2004) 4958–4971.
- [18] W.P. To, G.S.M. Tong, C.W. Cheung, C. Yang, D. Zhou, C.M. Che, Luminescent Cyclometalated Gold(III) Alkyl Complexes: Photophysical and Photochemical Properties, *Inorg. Chem.* 56 (2017) 5046–5059.
- [19] X. Wang, S. Goeb, Z. Ji, N.A. Pogulaichenko, F.N. Castellano, Homogeneous photocatalytic hydrogen production using π -conjugated platinum(II) arylacetylide sensitizers, *Inorg. Chem.* 50 (2011) 705–707.
- [20] D. Zhang, L.-Z. Wu, L. Zhou, X. Han, Q.-Z. Yang, L.-P. Zhang, C.-H. Tung, Photocatalytic Hydrogen Production from Hantzsch 1,4-Dihydropyridines by Platinum(II) Terpyridyl Complexes in Homogeneous Solution, *J. Am. Chem. Soc.* 126 (11) (2004) 3440–3441.
- [21] W.-Y. Wong, Z.e. He, S.-K. So, K.-L. Tong, Z. Lin, A Multifunctional Platinum-Based Triplet Emitter for OLED Applications #, *Organometallics* 24 (16) (2005) 4079–4082.
- [22] G. Konti, G.C. Vougioukalakis, M. Bidikoudi, A.G. Kontos, C. Methenitis, P. Falaras, A Ru(II) molecular antenna bearing a novel bipyridine-acrylonitrile ligand: Synthesis and application in dye solar cells, *Polyhedron* 82 (2014) 12–18.
- [23] H.Y. Shiu, H.C. Chong, Y.C. Leung, T. Zou, C.M. Che, Phosphorescent proteins for bio-imaging and site selective bio-conjugation of peptides and proteins with luminescent cyclometalated iridium(III) complexes, *Chem. Commun.* 50 (2014) 4375–4379.
- [24] P.H. Lanoë, J.L. Fillaut, L. Toupet, J.A.G. Williams, H. Le Bozec, V. Guerschais, Cyclometalated platinum(II) complexes incorporating ethynyl-flavone ligands: Switching between triplet and singlet emission induced by selective binding of Pb^{2+} ions, *Chem. Commun.* 4333–4335 (2008).
- [25] P.K.M. Siu, S.W. Lai, W. Lu, N. Zhu, C.M. Che, A diiminoplatinum(II) complex of 4-ethynylbenzo-15-crown-5 as a luminescent sensor for divalent metal ions, *Eur. J. Inorg. Chem.* 062 (2003) 2749–2752.
- [26] K.-H. Wong, M.-W. Chan, C.-M. Che, Modular Cyclometalated Platinum(II) Complexes as Luminescent Molecular Sensors for pH and Hydrophobic Binding Regions, *Chem. Eur. J.* 5 (10) (1999) 2845–2849.
- [27] S.W. Thomos, K. Venkatesan, P. Müller, T.M. Swager, Dark-field oxidative addition-based chemosensing: New bis-cyclometalated Pt(II) complexes and phosphorescent detection of cyanogen halides, *J. Am. Chem. Soc.* 128 (2006) 16641–16648.
- [28] R. Wai-Yin Sun, D.-L. Ma, E.-M. Wong, C.-M. Che, Some uses of transition metal complexes as anti-cancer and anti-HIV agents, *Dalton Trans.* (43) (2007) 4884, <https://doi.org/10.1039/b705079h>.
- [29] M. Ghedini, D. Pucci, A. Crispini, G. Barberio, Oxidative addition to cyclometalated azobenzene platinum(II) complexes: A route to octahedral liquid crystalline materials, *Organometallics* 18 (1999) 2116–2124.
- [30] Z. Guo, W.L. Tong, M.C.W. Chan, Luminescent oligo(ethylene glycol)-functionalized cyclometalated platinum(II) complexes: Cellular characterization and mitochondria-specific localization, *Chem. Commun.* 50 (2014) 1711–1714.
- [31] H. Schmidbaur, The fascinating implications of new results in gold chemistry, *Gold Bull* 23 (1) (1990) 11–21.
- [32] A. Bossi, A.F. Rausch, M.J. Leitl, R. Czerwieńiec, M.T. Whited, P.I. Djurovich, H. Yersin, M.E. Thompson, photophysical properties of cyclometalated Pt(II) complexes: Counterintuitive blue shift in emission with an expanded ligand π system, *Inorg. Chem.* 52 (2013) 12403–12415.
- [33] S. Verma, P. Kar, A. Das, H.N. Ghosh, Photophysical properties of ligand localized excited state in ruthenium(II) polypyridyl complexes: A combined effect of electron donor-acceptor ligands, *Dalton Trans.* 40 (2011) 9765–9773.
- [34] S.W. Lai, T.C. Cheung, M.C.W. Chan, K.K. Cheung, S.M. Peng, C.M. Che, Luminescent mononuclear and binuclear cyclometalated palladium(II) complexes of 6-phenyl-2,2'-bipyridines: Spectroscopic and structural comparisons with platinum(II) analogues 1,2, *Inorg. Chem.* 39 (2000) 255–262.
- [35] S.D. Cummings, R. Eisenberg, Tuning the excited-state properties of platinum (II) diamine dithiolate complexes, *J. Am. Chem. Soc.* 118 (1996) 1949–1960.
- [36] Wenfang Sun, Zi-Xin Wu, Qing-Zheng Yang, Li-Zhu Wu, Chen-Ho Tung, Reverse saturable absorption of platinum ter/bipyridyl polyphenylacetylide complexes, *Appl. Phys. Lett.* 82 (6) (2003) 850–852.
- [37] Arnold B. Tamayo, Bert D. Alleyne, Peter I. Djurovich, Sergey Lamansky, Irina Tsyba, Nam N. Ho, Robert Bau, Mark E. Thompson, Synthesis and Characterization of Facial and Meridional Tris-cyclometalated Iridium(III) Complexes, *J. Am. Chem. Soc.* 125 (24) (2003) 7377–7387.
- [38] M. Ray, D. Gosh, Z. Shirin, R. Mukherjee, Highly stabilized Low-spin Oron(III) and Cobalt(III) Complexes of a Tridentate Bis-Amide Ligand 2,6-Bis(N-phenylcarbomoyl)pyridine. Novel Nonmacrocyclic Tetramido-N Coordination and Two Unusually Short Metal-Pyridine Bonds, *Inorg. Chem.* 36 (1997) 3568–3572.
- [39] K. Sakai, Y. Tomita, T. Ue, K. Goshima, M. Ohminato, T. Tsubomura, K. Marsumoto, K. Ohmura, K. Kawakami, Syntheses, antitumor activity and molecular mechanics studies of cis-PtCl₂(pzH)₂ (pzH= pyrazole) and related complexes. Crystal structure of a novel Magnus-type double-salt [Pt(pzH)₄][PtCl₄][cis-PtCl₂(pzH)₂]₂ involving two perpendicularly aligned 1D cha, *Inorg. Chim. Acta.* 297 (2000) 64–71.
- [40] Takehiro Ochi, Yoshitaka Ohkubo, Seitaro Mutoh, FR143166 attenuates spinal pain transmission through activation of the serotonergic system, *Eur. J. Pharmacol.* 452 (3) (2002) 319–324.
- [41] R.H. Blessing, An empirical correction for absorption anisotropy, *Acta Crystallogr. Sect. A.* 51 (1995) 33–38.
- [42] George M. Sheldrick, A short history of SHELX, *Acta Crystallogr. A Found. Crystallogr.* 64 (1) (2008) 112–122.